2011 American Control Conference
on O'Farrell Street, San Francisco, CA, USA
June 29 - July 01, 2011

Active Disturbance Rejection Control for Human Postural Sway[1]

Radhika Kotina[2], Qing Zheng[3,*], *Senior Member, IEEE,* Antonie J. van den Bogert[4], and Zhiqiang Gao[5], *Member, IEEE*

***Abstract*—A fundamental and open issue pertaining to human postural sway is how to deal with the uncertain, nonlinear and time-varying nature of human motor dynamics. To address the inherent limitations of the current methods, such as PID and model-based designs, a novel active disturbance rejection concept is introduced. In this new framework, the uncertainties, nonlinearities and changes in the dynamics of the plant are treated as disturbance to be rejected. A unique disturbance rejection observer is employed to estimate it and compensate for it in real time. It is shown that the resulting new controller yields excellent performance even with significant uncertainties in the plant dynamics. Furthermore, such design strategy requires very little prior knowledge of the plant.**

Keywords— postural control; functional electrical stimulation; extended state observer; active disturbance rejection control

I. INTRODUCTION

Although people spend countless, seemingly effortless, hours standing during their lifetime, the task of maintaining balance is actually quite complex. To analyze this complex task of quiet standing, either ankle strategy or hip strategy can be used, with the former is usually used for small perturbations, and the latter for larger perturbations [1]. This paper will deal with ankle strategy, in which the body moves as a rigid mass around the ankle joints and hence is regarded as a single-link inverted pendulum with movement around the ankle joint.

Spinal cord injury results in an interruption of the neurological pathway from brain to muscles. A complete lesion of the spinal cord in the back (thoriac level) results in the paralysis of lower limbs and loss of voluntary control of the muscles below the level of lesion. Paralyzed muscles do however retain their ability to contract, and they can be simulated by extraneous electrical signals, which can be used for therapeutic purposes. The ultimate goal in therapy is to restore postural balance artificially by stimulation of the ankle muscles in a way analogous to the mode in which normal people stand. Towards this goal, we need first to understand how muscles generate forces under stimulation, i.e. the dynamics of the muscle. Based on this understanding, we need to design a control system that will provide the appropriate muscle stimulation signals to keep the person from losing balance.

The pragmatic nature of this effort requires that a realistic and nonlinear model of ankle joint to be used, instead of the simplistic linear approximations commonly seen in literature concerning the control of postural sway. It is well-known that the real muscles are quite complex, nonlinear and time-varying in nature. A more realistic musculoskeletal model of this ankle joint would be crucial in understanding the muscle dynamics and in evaluating the performance of the controller that can provide artificial balance for the paraplegic patients. A control strategy must be devised to accommodate the nature of human postural sway that is unknown or uncertain in many ways. Many existing techniques may not be suitable for the human postural control problem because they require accurate mathematical model of the plant, which is usually unavailable.

A survey of control strategies for human postural sway has been given in [2]. Feedforward and open-loop control have been employed for functional electrical stimulation (FES) systems [3-5]. In these methods, stimulation parameters are calculated by the controller to generate a desired movement. Feedforward control has been used for various purposes, such as upper extremity movement including hand grasp [6-7], single-joint arm movements [8], and elbow extension [9]. It does not require sensors, which facilitates rapid movements and greatly simplifies controller implementation in humans. By itself, however, no corrections can be made if the actual movement deviates from the desired one and it requires a detailed system behavior [10]. Another class of approaches is feedback control. Feedback control has been extensively used for many FES applications [4, 10-13]. It uses sensors to monitor the output and to have the output behave as the desired one [10]. However, feedback control in clinical applications has been limited due to the requirement of body-mounted sensors [14]. The challenges come from the sensor signal quality and inherent delays in system response [4, 15]. Other advanced FES feedback controllers were investigated incorporating various techniques, such as combination of feedforward and feedback control [16, 17], reinforcement learning [18, 19], and artificial neural networks [20-22]. However, the tuning of these approaches is nontrivial, especially for nonlinear processes in the presence of significant dynamic uncertainties and disturbances [23-28].

The purpose of this paper is to provide a practical solution, based on the active disturbance rejection concept, to the human posture control problem and show analytically how

[1]The work was sponsored in part by the Faculty Development Grant of Gannon University under Grant 10-1-0000-21495.
[2]Honeywell International Inc., 21111 N. 19th Avenue, Phoenix, AZ 85027.
[3]Department of Electrical and Computer Engineering, Gannon University, Erie, PA 16541.
[4]Orchard Kinetics LLC, 2217 S. Overlook Rd, Cleveland Heights, OH 44106.
[5]Department of Electrical and Computer Engineering, Cleveland State University, Cleveland, Ohio 44115.
[*]Corresponding author. Tel.: +1-814-871-5617; fax: +1-814-871-7616. E-mail: zheng003@gannon.edu.

this novel control technology achieves excellent performance for the uncertain, nonlinear, and time-varying dynamic systems. The stability characteristics of the proposed control approach is also analyzed.

This paper is organized as follows. The nonlinear simulation model for human postural sway is discussed in Section II. The active disturbance rejection control design strategy is introduced in Section III. Comparison of different control approaches for systems with significant dynamic variations and external disturbances is presented in Section IV. Finally, some concluding remarks are given in Section V.

II. Nonlinear Simulation Model

The human pastoral sway model considered in this paper is shown in Fig. 1. It includes the muscle properties which are interactively complex, but contribute substantially to the dynamic stability of the musculoskeletal system, as shown by Gerritsen *et al.* [29]. The ankle joint has three muscles, Tibialis Anterior at the front, Gastrocnemius and Soleus at the back. Gastrocnemius and Soleus can be combined into one as Triceps Surae muscle. This is valid as the knee is locked and so it does not make a difference that Gastrocnemius is a two-joint muscle.

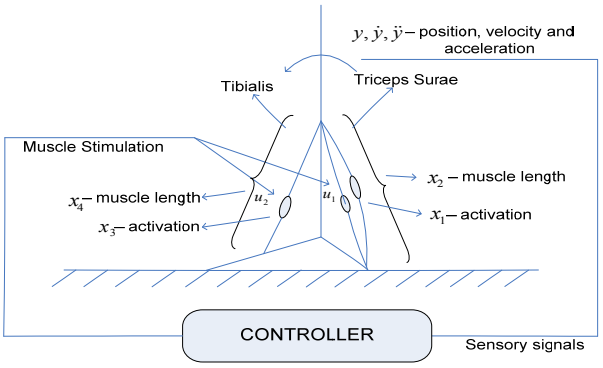

Fig. 1. The human pastoral sway model using ankle strategy.

Each muscle tendon is modeled as a three-component hill model and the muscle properties are taken from the work by McLean *et al.* [30]. Muscle activation dynamics was modeled as a first order differential equation. The model used here is taken from the cat's hind limb model and replaced with the human ankle parameters.

To describe the model in short, when muscle stimulation is given as an input to a muscle, it passes through a first order filter and results in the activation. This activation affects the force length relationship leading to the change in length, which in turn produces force in the muscle. The total force affects the acceleration of the ankle and hence the position. A Simulink model is developed and the block diagram is shown in Fig. 2.

From the open loop response (not shown here for brevity), it can be determined that the ankle joint represented by this model can lean in the forward direction by a maximum of 18.5° as the foot is locked to the ground. Similarly, it can

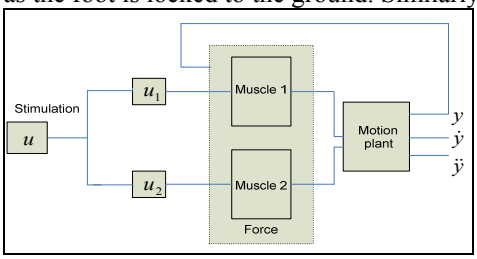

Fig. 2. The open-loop Simulink model block diagram.

lean backward by a maximum of 1.35°. Beyond these limits, there is not enough muscle strength to recover the joint to the vertical direction (0° lean). In practice, when the ankle joint exceeds a limit of around 8° and 1° in forward and backward directions, the hip strategy comes into picture. For the sake of simplicity, the hip strategy is ignored in the present paper, as the performance of the control system is of the main interest. For this purpose, it is assumed that the foot is locked to the ground and the maximum sway that the ankle joint can attain, among other performance considerations, is an important characteristic of closed-loop control system.

The present model of the plant is highly nonlinear and time-varying with significant uncertainties, caused by dynamic variations in human muscles. These characteristics make model based control designs such as pole placement, feedback linearization, sliding model control and H_2/H_∞ control not feasible for this problem. Therefore the active disturbance rejection control (ADRC), which does not depend on accurate mathematical model, is proposed.

III. Active Disturbance Rejection Control

The basic idea of the ADRC is to take the combination of internal dynamics and external disturbance of the system as the total disturbance and actively reject it in the control law. The concept of ADRC is introduced below.

A. Active Disturbance Rejection Concept

The general motion problem can be formulated as

$$\ddot{y}(t) = f\left(y(t), \dot{y}(t), d_t(t)\right) + bu(t) \tag{1}$$

where y is the output position, and u is the control signal, d_t refers to the total disturbance including linear and nonlinear disturbances with unknown characteristics, the generalized nonlinear function $f(.)$, simply denoted as f, represents the combined effect of internal dynamics and external disturbances. The concept of active disturbance rejection is if

$$f = \ddot{y} - bu \tag{2}$$

can be measured or estimated, the control law

$$u = (u_0 - f)/b \tag{3}$$

reduces the plant (1) to a simple double integral plant. Initially, assume all the three states, position, velocity, and acceleration, are measurable, then we have

$$\ddot{y} = \left(f + b\frac{(u_0 - f)}{b} \right) = u_0 \tag{4}$$

which can be easily controlled by a PD controller. This design strategy proves to be effective for the human posture control, as shown later. In reality, the muscle model is more complex than depicted in (1) with additional state variables and highly nonlinear functions. In the above ADRC concept, most of this complexity can be treated as uncertainty, estimated in real time and canceled, making control design task a much simpler one. In practice, the acceleration signal is required for control. An accelerometer can be used on the patient's belt to measure this signal [31]. The ADRC provides a similar functionality to acceleration feedback control. With the novel active disturbance rejection concept, a unique observer, extended state observer (ESO), is proposed to estimate f in real time [32–34]. The concept of ESO is presented below.

B. Extended State Observer Design

Let $\xi_1 = y, \xi_2 = \dot{y}, \xi_3 = f$ and $\xi = [\xi_1 \quad \xi_2 \quad \xi_3]^T$. Assuming f is differentiable, the state space form of (1) is

$$\begin{cases} \dot{\xi} = A\xi + Bu + Eh \\ y = C\xi \end{cases} \tag{5}$$

where $A = \begin{bmatrix} 0 & 1 & 0 \\ 0 & 0 & 1 \\ 0 & 0 & 0 \end{bmatrix}, B = \begin{bmatrix} 0 \\ b \\ 0 \end{bmatrix}, C = \begin{bmatrix} 1 & 0 & 0 \end{bmatrix}, E = \begin{bmatrix} 0 \\ 0 \\ 1 \end{bmatrix}$, $\xi_3 = f$ is the augmented state, and $h = \dot{f}$. A continuous ESO for (5) is designed as

$$\begin{cases} \dot{\hat{\xi}} = A\hat{\xi} + Bu + L(y - \hat{y}) \\ \hat{y} = C\hat{\xi} \end{cases} \tag{6}$$

where $L = \begin{bmatrix} l_1 & l_2 & l_3 \end{bmatrix}^T$ is the observer gain vector. The observer gains are chosen such that the characteristic polynomial $s^3 + l_1 s^2 + l_2 s + l_3$ is Hurwitz. For tuning simplicity, all the observer poles are placed at $-\omega_o$. It results in the characteristic polynomial of (6) to be

$$\lambda_o(s) = s^3 + l_1 s^2 + l_2 s + l_3 = (s + \omega_o)^3 \tag{7}$$

where ω_o is the observer bandwidth and $L = \begin{bmatrix} 3\omega_o & 3\omega_o^2 & \omega_o^3 \end{bmatrix}^T$.

C. Control Algorithm

Once the observer is designed and well tuned, its outputs will track ξ_1, ξ_2, and ξ_3 respectively. By canceling the effect of f using $\hat{\xi}_3$, ADRC actively compensates for f in real time. The ADRC control law is given by

$$u = \frac{k_1\left(r - \hat{\xi}_1\right) + k_2\left(\dot{r} - \hat{\xi}_2\right) - \hat{\xi}_3 + \ddot{r}}{b} \tag{8}$$

where r is the desired trajectory, k_1 and k_2 are the controller gain parameters selected to make $s^2 + k_2 s + k_1$ Hurwitz. For simplicity, let $k_1 = \omega_c^2$, $k_2 = 2\omega_c$, where ω_c is the controller bandwidth. The closed-loop system for the system (1) becomes

$$\ddot{y} = \left(f - \hat{\xi}_3\right) + k_1\left(r - \hat{\xi}_1\right) + k_2\left(\dot{r} - \hat{\xi}_2\right) + \ddot{r}. \tag{9}$$

Note that with a well-designed ESO, the first term in the right hand side (RHS) of (9) is negligible and the rest of the terms in the RHS of (9) constitute a PD controller with a feedforward gain.

The convergence for the estimation error of the ESO and the closed-loop tracking error of ADRC is shown below.

D. Stability

1) Convergence of the ESO

Let $\tilde{\xi}_i(t) = \xi_i(t) - \hat{\xi}_i(t)$, $i = 1, 2, 3$. From (5) and (6), the observer estimation error dynamics can be shown as

$$\begin{aligned} \dot{\tilde{\xi}}_1 &= \tilde{\xi}_2 - l_1\tilde{\xi}_1 \\ \dot{\tilde{\xi}}_2 &= \tilde{\xi}_3 - l_2\tilde{\xi}_1 \\ \dot{\tilde{\xi}}_3 &= h - l_3\tilde{\xi}_1. \end{aligned} \tag{10}$$

Now let us scale the observer estimation error $\tilde{\xi}_i(t)$ by ω_o^{i-1}, i.e., let $\varepsilon_i(t) = \frac{\tilde{\xi}_i(t)}{\omega_o^{i-1}}, i = 1, 2, 3.$ Then (10) can be rewritten as

$$\dot{\varepsilon} = \omega_o A_\varepsilon \varepsilon + B_\varepsilon \frac{h(\xi, d_t)}{\omega_o^2} \tag{11}$$

where $A_\varepsilon = \begin{bmatrix} -3 & 1 & 0 \\ -3 & 0 & 1 \\ -1 & 0 & 0 \end{bmatrix}, B_\varepsilon = \begin{bmatrix} 0 \\ 0 \\ 1 \end{bmatrix}$.

Theorem 1: Assuming $h(\xi, d_t)$ is bounded, then there exist a constant $\sigma_i > 0$ and a finite time $T_1 > 0$ such that $\left|\tilde{\xi}_i(t)\right| \le \sigma_i$, $i = 1, 2, 3$, $\forall t \ge T_1 > 0$ and $\omega_o > 0$. Furthermore, $\sigma_i = \mathrm{O}\left(\frac{1}{\omega_o^k}\right)$, for some positive integer k.

Proof: Solving (11), we can obtain

$$\varepsilon(t) = e^{\omega_o A_\varepsilon t}\varepsilon(0) + \int_0^t e^{\omega_o A_\varepsilon (t-\tau)} B_\varepsilon \frac{h(\xi(\tau), d_t)}{\omega_o^2} d\tau. \tag{12}$$

Let

$$p(t) = \int_0^t e^{\omega_o A_\varepsilon (t-\tau)} B_\varepsilon \frac{h(\xi(\tau), d_t)}{\omega_o^2} d\tau. \tag{13}$$

Since $h(\xi(\tau), d_t)$ is bounded, that is, $\left|h(\xi(\tau), d_t)\right| \le \delta$, where δ is a positive constant, it follows that

$$\left|p_i(t)\right| \le \frac{\delta}{\omega_o^3}\left[\left|\left(A_\varepsilon^{-1} B_\varepsilon\right)_i\right| + \left|\left(A_\varepsilon^{-1} e^{\omega_o A_\varepsilon t} B_\varepsilon\right)_i\right|\right] \tag{14}$$

for $i = 1, 2, 3$. Since $A_\varepsilon^{-1} = \begin{bmatrix} 0 & 0 & -1 \\ 1 & 0 & -3 \\ 0 & 1 & -3 \end{bmatrix}$, One has

$$\left|\left(A_\varepsilon^{-1} B\right)_i\right| = \begin{cases} 1\big|_{i=1} \\ 3\big|_{i=2,3} \end{cases}. \tag{15}$$

Since A_ε is Hurwitz, there exists a finite time $T_1 > 0$ such that

$$\left|\left[e^{\omega_o A_\varepsilon t}\right]_{ij}\right| \le \frac{1}{\omega_o^3} \tag{16}$$

for all $t \ge T_1$, $i, j = 1,2,3$. Hence

$$\left|\left[e^{\omega_o A_\varepsilon t} B\right]_i\right| \le \frac{1}{\omega_o^3} \tag{17}$$

for all $t \ge T_1$, $i = 1,2,3$. Note that T_1 depends on $\omega_o A_\varepsilon$. Let $A_\varepsilon^{-1} = \begin{bmatrix} s_{11} & s_{12} & s_{13} \\ s_{21} & s_{22} & s_{23} \\ s_{31} & s_{32} & s_{33} \end{bmatrix}$ and $e^{\omega_o A_\varepsilon t} = \begin{bmatrix} d_{11} & d_{12} & d_{13} \\ d_{21} & d_{22} & d_{23} \\ d_{31} & d_{32} & d_{33} \end{bmatrix}$.

One has

$$\begin{aligned} \left|\left(A_\varepsilon^{-1} e^{\omega_o A_\varepsilon t} B_\varepsilon\right)_i\right| &= \left|s_{i1} d_{13} + s_{i2} d_{23} + s_{i3} d_{33}\right| \\ &\le \begin{cases} \left|\dfrac{1}{\omega_o^3}\right|_{i=1} \\ \left|\dfrac{4}{\omega_o^3}\right|_{i=2,3} \end{cases} \end{aligned} \tag{18}$$

for all $t \ge T_1$. From (14), (15) and (18), we obtain

$$\left|p_i(t)\right| \le \frac{3\delta}{\omega_o^3} + \frac{4\delta}{\omega_o^6} \tag{19}$$

For all $t \ge T_1, i = 1,2,3$. Let $\varepsilon_{sum}(0) = \left|\varepsilon_1(0)\right| + \left|\varepsilon_2(0)\right| + \left|\varepsilon_3(0)\right|$. It follows that

$$\left|\left[e^{\omega_o A_\varepsilon t} \varepsilon(0)\right]_i\right| \le \frac{\varepsilon_{sum}(0)}{\omega_o^3} \tag{20}$$

for all $t \ge T_1$, $i = 1,2,3$. From (12), one has

$$\left|\varepsilon_i(t)\right| \le \left|\left[e^{\omega_o A_\varepsilon t} \varepsilon(0)\right]_i\right| + \left|p_i(t)\right|. \tag{21}$$

Let $\tilde{\xi}_{sum}(0) = \left|\tilde{\xi}_1(0)\right| + \left|\tilde{\xi}_2(0)\right| + \left|\tilde{\xi}_3(0)\right|$. According to $\varepsilon_i(t) = \dfrac{\tilde{\xi}_i(t)}{\omega_o^{i-1}}$ and (19)-(21), we have

$$\begin{aligned} \left|\tilde{\xi}_i(t)\right| &\le \left|\frac{\tilde{\xi}_{sum}(0)}{\omega_o^3}\right| + \frac{3\delta}{\omega_o^{4-i}} + \frac{4\delta}{\omega_o^{7-i}} \\ &= \sigma_i \end{aligned} \tag{22}$$

for all $t \ge T_1$, $i = 1,2,3$. Q.E.D.

It is shown above that in the absence of the plant model, the estimation error of the ESO (6) is bounded and its upper bound monotonously decreases with the observer bandwidth.

The convergence of ADRC, where ESO is employed, is analyzed next.

2) Convergence of the ADRC

Let $\left[r_1, r_2, r_3\right]^T = \left[r, \dot{r}, \ddot{r}\right]^T$ and $e_i(t) = r_i(t) - \xi_i(t)$, $i = 1,2$.

Theorem 2: Assuming that h is bounded, there exist a constant $\rho_i > 0$ and a finite time $T_3 > 0$ such that $\left|e_i(t)\right| \le \rho_i$, $i = 1,2, \forall t \ge T_3 > 0, \omega_o > 0$ and $\omega_c > 0$. Furthermore, $\rho_i = \mathrm{O}\left(\dfrac{1}{\omega_c^q}\right)$ for some positive integer q .

Proof: From (8), one has

$$u = \frac{k_1\left(e_1 + \tilde{\xi}_1\right) + k_2\left(e_2 + \tilde{\xi}_2\right) - \left(\xi_3 - \tilde{\xi}_3\right) + r_3}{b}. \tag{23}$$

It follows that

$$\begin{aligned} \dot{e}_1 &= \dot{r}_1 - \dot{\xi}_1 = r_2 - \xi_2 = e_2 \\ \dot{e}_2 &= -k_1\left(e_1 + \tilde{\xi}_1\right) - k_2\left(e_2 + \tilde{\xi}_2\right) - \tilde{\xi}_3. \end{aligned} \tag{24}$$

Let $e(t) = \left[e_1(t), e_2(t)\right]^T$, $\tilde{\xi}(t) = \left[\tilde{\xi}_1(t), \tilde{\xi}_2(t), \tilde{\xi}_3(t)\right]^T$, then

$$\dot{e}(t) = A_e e(t) + A_{\tilde{\xi}} \tilde{\xi}(t) \tag{25}$$

where $A_e = \begin{bmatrix} 0 & 1 \\ -k_1 & -k_2 \end{bmatrix}$ and $A_{\tilde{\xi}} = \begin{bmatrix} 0 & 0 & 0 \\ -k_1 & -k_2 & -1 \end{bmatrix}$.

Solving (25), we have

$$e(t) = e^{A_e t} e(0) + \int_0^t e^{A_e(t-\tau)} A_{\tilde{\xi}} \tilde{\xi}(\tau)\, d\tau. \tag{26}$$

According to (25) and Theorem 1, one has

$$\begin{aligned} &\left[A_{\tilde{\xi}} \tilde{\xi}(\tau)\right]_{i=1} = 0 \\ &\left|\left[A_{\tilde{\xi}} \tilde{\xi}(\tau)\right]_2\right| \le k_{sum}\sigma = \gamma \text{ for all } t \ge T_1 \end{aligned} \tag{27}$$

where $k_{sum} = 1 + k_1 + k_2$. Let $\varphi(t) = \int_0^t e^{A_e(t-\tau)} A_{\tilde{\xi}} \tilde{\xi}(\tau)\, d\tau$.

Define $\Psi = \begin{bmatrix} 0 & \gamma \end{bmatrix}^T$. It follows that

$$\left|\varphi_i(t)\right| \le \left|\left(A_e^{-1}\Psi\right)_i\right| + \left|\left(A_e^{-1} e^{A_e t}\Psi\right)_i\right|; \tag{28}$$

and

$$\begin{aligned} \left|\left(A_e^{-1}\Psi\right)_1\right| &= \frac{\gamma}{\omega_c^2} \\ \left|\left(A_e^{-1}\Psi\right)_2\right| &= 0. \end{aligned} \tag{29}$$

Since A_e is Hurwitz, there exists a finite time $T_2 > 0$ such that

$$\left|\left[e^{A_e t}\right]_{ij}\right| \le \frac{1}{\omega_c^3} \tag{30}$$

for all $t \ge T_2$, $i, j = 1,2$. Note that T_2 depends on A_e. Let $e^{A_e t} = \begin{bmatrix} o_{11} & o_{12} \\ o_{21} & o_{22} \end{bmatrix}$ and $e_{sum}(0) = \left|e_1(0)\right| + \left|e_2(0)\right|$. It follows that

$$\left|\left[e^{A_e t} e(0)\right]_i\right| \le \frac{e_{sum}(0)}{\omega_c^3} \tag{31}$$

for all $t \ge T_2$, $i = 1,2$. Let $T_3 = \max\left\{T_1, T_2\right\}$. We have

$$\left|\left(e^{A_e t}\Psi\right)_i\right| \le \frac{\gamma}{\omega_c^3} \tag{32}$$

for all $t \ge T_3$, $i = 1,2$, and

$$\left|\left(A_e^{-1} e^{A_e t}\Psi\right)_i\right| \le \begin{cases} \left|\dfrac{1 + 2\omega_c}{\omega_c^2}\dfrac{\gamma}{\omega_c^3}\right|_{i=1} \\ \left|\dfrac{\gamma}{\omega_c^3}\right|_{i=2} \end{cases} \tag{33}$$

for all $t \ge T_3$. From (28), (29), and (33), we obtain

$$|\varphi_i(t)| \le \begin{cases} \left| \frac{\gamma}{\omega_c^2} + \frac{1+2\omega_c}{\omega_c^2}\frac{\gamma}{\omega_c^3} \right|_{i=1} \\ \left| \frac{\gamma}{\omega_c^3} \right|_{i=2} \end{cases} \quad (34)$$

for all $t \ge T_3$. From (26), one has

$$|e_i(t)| \le \left| \left[e^{A_e t} e(0) \right]_i \right| + |\varphi_i(t)|. \quad (35)$$

According to (31), (34)-(35), we have

$$|e_i(t)| \le \begin{cases} \left| \frac{e_{sum}(0)}{\omega_c^3} + \frac{(1+2\omega_c+\omega_c^2)\sigma_i}{\omega_c^2} + \frac{(1+2\omega_c+\omega_c^2)(1+2\omega_c)\sigma_i}{\omega_c^5} \right|_{i=1} \\ \left| \frac{e_{sum}(0)+(1+2\omega_c+\omega_c^2)\sigma_i}{\omega_c^3} \right|_{i=2} \end{cases} \quad (36)$$

$$\le \rho_i$$

for $t \ge T_3$, $i = 1, 2$, where

$$\rho_i = \max\left\{ \frac{e_{sum}(0)}{\omega_c^3} + \frac{(1+2\omega_c+\omega_c^2)\sigma_i}{\omega_c^2} + \frac{(1+2\omega_c+\omega_c^2)(1+2\omega_c)\sigma_i}{\omega_c^5}, \frac{e_{sum}(0)+(1+2\omega_c+\omega_c^2)\sigma_i}{\omega_c^3} \right\}.$$

Q.E.D.

It has been shown above that, with plant dynamics largely unknown, the closed-loop tracking error and its derivative are bounded and their upper bounds monotonously decrease with the observer and controller bandwidths. With the convergence of ESO and ADRC established, we now present the simulation test results.

IV. Comparative Study

In this section, the simulation results of ADRC and PID are used to evaluate their performance in the presence of dynamic uncertainties and disturbances. Both ADRC with direct measurement of states and ADRC with ESO are tested. Three cases are tested for the human postural system with the reference signal of 0 degree and the simulation results are shown in Fig. 3. Fig. 3(a) shows the performance of the three controllers under nominal condition, with the initial condition set at the angle of 0 degree. Fig. 3(b) shows the performance of the three controllers when the inertia is reduced by a factor of four. Fig. 3 (c) shows the performance of the three controllers when an external force of 20 Nm is introduced at t=12 s.

The simulation results show that both ADRC with direct measurement and ADRC with ESO achieve high performance of robustness and disturbance rejection in the presence of dynamic uncertainty and external disturbances. Under the nominal condition of 0 degree reference, the ADRC with direct measurement shows the least amount of overshoot. Both ADRC approaches have small overshoots and the settling time of around 4 seconds, while it takes PID 8 seconds to reach the steady state with a larger overshoot. When the inertia is decreased, ADRC approaches provide consistent responses without adjusting the tuning parameters. However, PID performs an oscillatory response, which indicates that it is sensitive to parameter variations. Fig. 3(c) demonstrates the excellent disturbance rejection performance of ADRC technology. Note that the maximum disturbance that ADRC approaches can tolerate is 100 Nm at a non-zero reference of 4°, while PID can tolerate no more than 60 Nm.

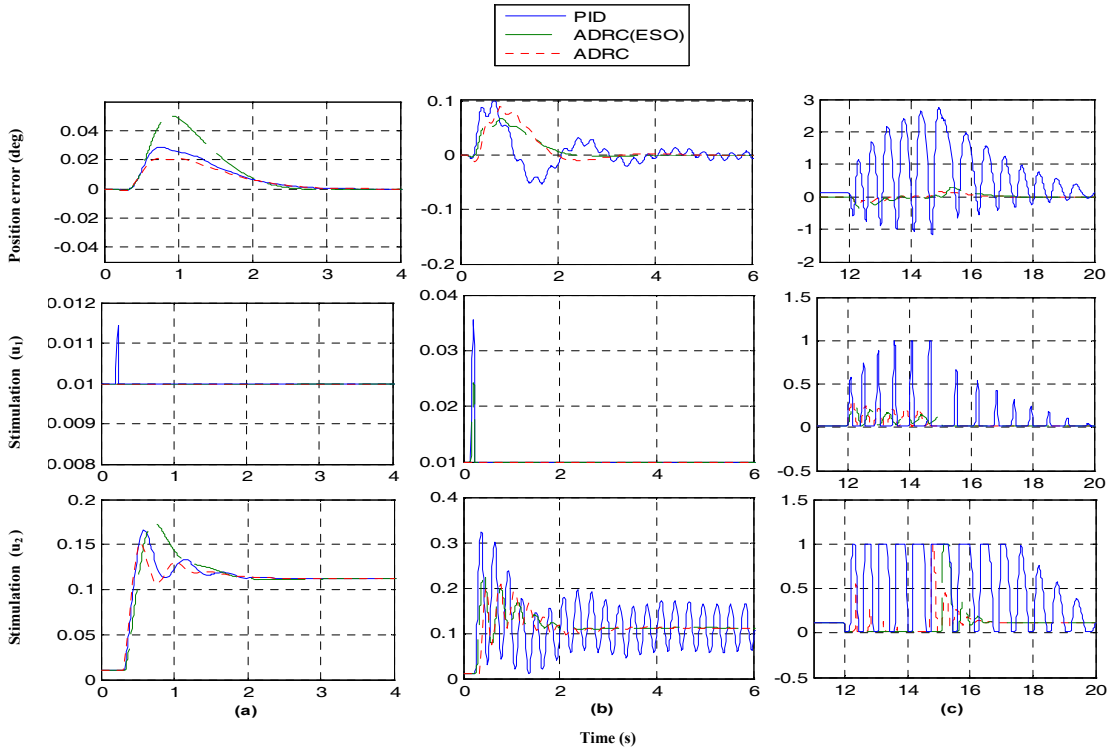

Fig. 3. (a) nominal condition, (b) with decreased inertia, (c) with a push of 20 Nm at t = 12 s.

V. Concluding Remarks

In this paper, a Simulink model is developed for a nonlinear dynamic ankle joint from a set of differential equations. A novel control concept, active disturbance rejection, is successfully applied to solve the human pastoral control problem with the uncertain, nonlinear, and time-varying nature of human motor dynamics. Stability analysis shows that the boundedness of the estimation and closed-loop tracking errors is assured. Furthermore, it is established that the error upper bounds monotonously decrease with the bandwidths. Simulation results demonstrate the effectiveness of the ADRC.

References

[1] A. D. Kuo and F. E. Zajac, "Human standing posture: multi-joint movement strategies based on biomechanical constraints," *Progress in Brain Research*, vol. 97, pp. 349-358, 1993.

[2] K. M. Jagodnik and A. J. van den Bogert, "Optimization and evaluation of a proportional derivative controller for planar arm movement," *Journal of Biomechanics*, vol. 43, no. 6, pp. 1086-1091, 2010.

[3] D. Blana, R. F. Kirsch, and E. K. Chadwick, "Combined feedforward and feedback control of are Dunant, nonlinear, dynamic musculoskeletal system," *Medical & Biological Engineering & Computing*, Special Issue-Review, vol. 47, no. 5, pp. 533–542, 2009.

[4] J. J. Abbas and R. J. Triolo, "Experimental evaluation of an adaptive feedforward controller for use in functional neuromuscular stimulation systems," *IEEE Transactions on Rehabilitation Engineering,* vol. 5, no. 1, pp. 12–22, 1997.

[5] K. L. Kilgore, P. H. Peckham, G. B. Thrope, M. W. Keith, and K. A. Gallaher-Stone, "Synthesis of hand grasp using functional neuromuscular stimulation," *IEEE Transactions on Biomedical Engineering*, vol. 36, no. 7, pp. 761–770, 1989.

[6] M. W. Keith, P. H. Peckham, G. B. Thrope, K. C. Stroh, B. Smith, J. R. Buckett, K. L. Kilgore, and J. W. Jatich, "Implantable functional neuromuscular stimulation in the tetraplegic hand," *Journal of Hand Surgery*, vol. 14, no. 3, pp. 524–530, 1989.

[7] K. H. Mauritz and P. H. Peckham, "Restoration of grasping functions in quadriplegic patients by Functional Electrical Stimulation (FES)," *International Journal of Rehabilitation Research*, vol. 10, no. 4, pp. 57–61, 1987.

[8] N. Lan and P. E. Crago, "Optimal control of antagonistic muscle stiffness during voluntary movements," *Biological Cybernetics*, vol. 71, no. 2, pp. 123–135, 1994.

[9] P. E. Crago, W. D. Memberg, M. K. Usey, M. W. Keith, R. F. Kirsch, G. J. Chapman, M. A. Katorgi, and E. J. Perreault, "An elbow extension neuroprosthesis for individuals with tetraplegia," *IEEE Transactions on Rehabilitation Engineering*, vol. 6, no. 1, pp. 1–6, 1998.

[10] P. E. Crago, N. Lan, P. H. Veltink, J. J. Abbas, and C. Kantor, "New control strategies for neuroprosthetic systems," *Journal of Rehabilitation Research and Development,* vol. 33, no. 2, pp. 158–172, 1996.

[11] P. E. Crago, R. J. Nakai, and H. J. Chizeck, "Feedback regulation of hand grasp opening and contact force during stimulation of paralyzed muscle," *IEEE Transactions on Biomedical Engineering*, vol. 38, no. 1, pp. 17–28, 1991.

[12] M. A. Lemay and P. E. Crago, "Closed-loop wrist stabilization in C4 and C5 tetraplegia," *IEEE Transactions on Rehabilitation Engineering*, vol. 5, no. 3, pp. 244–252, 1997.

[13] J. P. Giuffrida and P. E. Crago, "Reciprocal EMG control of elbow extension by FES," *IEEE Transactions on Neural Systems and Rehabilitation Engineering*, vol. 9, no. 4, pp. 338–345, 2001.

[14] H. J. Chizeck, R. Kobetic, E. B. Marsolais, J. J. Abbas, I. H. Donner, and E. Simon, "Control of functional neuromuscular stimulation systems for standing and locomotion in paraplegics," *Proceedings of the IEEE*, vol. 76, no. 9, pp. 1155–1165, 1988.

[15] S. Stroeve, "Learning combined feedback and feedforward control of a musculoskeletal system," *Biological Cybernetics*, vol. 75, no. 1, pp. 73–83, 1996.

[16] K. Kurosawa, R., Futami, T. Watanabe, and N. Hoshimiya, "Joint angle control by FES using a feedback error learning controller," *IEEE Transactions on Neural Systems and Rehabilitation Engineering,* vol. 13, no. 3, pp. 359–371, 2005.

[17] J. J. Abbas and H. J. Chizeck, "Neural network control of functional neuromuscular stimulation systems: computer simulation studies," *IEEE Transactions on Biomedical Engineering,* vol. 42, no. 11, pp. 1117–1127, 1995.

[18] P. Thomas, M. Branicky, A. J. van den Bogert, and K. Jagodnik, "Application of the actor–critic architecture to functional electrical stimulation control of a human arm," *Proceedings of the Twenty-First Innovative Applications of Artificial Intelligence Conference*, Pasadena, CA, USA, 2009.

[19] J. Izawa, T. Kondo, and K. Ito, "Biological arm motion through reinforcement learning," *Biological Cybernetics*, vol. 91, no. 1, pp. 10–22, 2004.

[20] S. D. Iftime, L. L. Egsgaard, and M. B. Popovic, "Automatic determination of synergies by radial basis function artificial neural networks for the control of a neural prosthesis," *IEEE Transactions on Neural Systems and Rehabilitation Engineering*, vol. 13, no. 4, pp. 482–489, 2005.

[21] J. P. Giuffrida and P. E. Crago, "Functional restoration of elbow extension after spinal-cord injury using a neural network-based synergistic FES controller," *IEEE Transactions on Neural Systems and Rehabilitation Engineering*, vol. 13, no. 2, pp. 147–152, 2005.

[22] J. Winslow, P. L. Jacobs, and D. Tepavac, "Fatigue compensation during FES using surface EMG," *Journal of Electromyography and Kinesiology*, vol. 13, no. 6, pp. 555–568, 2003.

[23] H. Dou, K. K. Tan, T. H. Lee, and Z. Zhou, "Iterative learning feedback control of human limbs via functional electrical stimulation," *Control Engineering Practice*, vol. 7, no. 3, pp. 315–325, 1999.

[24] J. Reiss and J. J. Abbas, "Adaptive neural network control of cyclic movements using functional neuromuscular stimulation," *IEEE Transactions on Rehabilitation Engineering*, vol. 8, no. 1, pp. 42–52, 2000.

[25] K. J. Astrom and T. Hagglund, "Revisiting the Ziegler–Nichols step response method for PID control," *Journal of Process Control,* vol. 14, pp. 635–650, 2004.

[26] K. L. Chien, J. A. Hrones, and J. B. Reswick, "On the automatic control of generalized passive systems," *Transactions of the ASME*, vol. 74, pp. 175–185, 1972.

[27] K. J. Astrom and T. Hagglund, "The future of PID control," *Control Engineering Practice*, vol. 9, no. 11, pp. 1163–1175, 2001.

[28] C. Dey and R. K. Mudi, "An improved auto-tuning scheme for PID controllers," *ISA Transactions*, vol. 48, no. 4, pp. 396–409, 2009.

[29] K. G. M. Gerritsen, A. J. van den Bogert, M. Hulliger, and R. F. Zernizke, "Intrinsic muscle properties facilitate locomotor control – a computer simulation study," Motor Control, *Human Kinematic Publishers, Inc.*, vol. 2, pp. 206-220, 1998.

[30] S. G. McLean, A. Su, and A. J. van den Bogert, "Development and validation of a 3-D model to predict knee joint loading during dynamic movement," *Transactions of the ASME*, vol. 125, no. 6, pp. 864-874, 2003.

[31] R. Nataraj, M. L. Audu, R. F. Kirsch, and R. J. Triolo, "Developing an artificial neural network controller for automated standing balance using functional neuromuscular stimulation following spinal cord injury," *Proceedings of Dynamic Walking, Mechanics and Control of Human and Robot Locomotion*, p. 51, Ann Arbor, MI, USA, May 6-8, 2006.

[32] Z. Gao, "Scaling and parameterization based controller tuning," *Proceedings of the 2003 American Control Conference*, pp. 4989-4996, 2003.

[33] Q. Zheng and Z. Gao, "Motion control design optimization: problem and solutions," *International Journal of Intelligent Control and Systems*, vol. 10, no. 4, pp. 269-276, 2006.

[34] Q. Zheng, Z. Chen, and Z. Gao, "A practical approach to disturbance decoupling control," *Control Engineering Practice,* vol. 17, no. 9, pp. 1016-1025, 2009.